Bollettino di Geofisica Teorica ed Applicata Vol. 52, n. 3, pp. 471-490; September 2011
DOI 10.4430/bgta0032

Characteristics of strong ground motions from the L'Aquila (M_w = 6.3) earthquake and its strongest aftershocks

F. Pacor[1], G. Ameri[1], D. Bindi[1], L. Luzi[1], M. Massa[1], R. Paolucci[2] and C.Smerzini[2]

[1] *Istituto Nazionale di Geofisica e Vulcanologia, Milano, Italy*
[2] *Dept. of Structural Engineering, Politecnico di Milano, Italy*

(Received: April 12, 2010; accepted: October 15, 2010)

ABSTRACT Strong motion data during the L'Aquila seismic sequence, were mainly recorded by the Italian accelerometric network (Rete Accelerometrica Nazionale, RAN), operated by the Department of Civil Protection (DPC). Several records were obtained also by a temporary network installed the day after the mainshock by the Istituto Nazionale di Geofisica e Vulcanologia (INGV). The L'Aquila earthquake is the third strongest seismic event producing strong-motion records in Italy, after the Irpinia (1980, M_w 6.9) and Friuli (1976, M_w 6.4) earthquakes. This event, together with its largest aftershocks ($M_w > 4.0$) provided a unique strong-motion data set in Italy, especially due to the amount and intensity of near-fault records. The data set included in the Italian strong motion database, ITACA, consists of about 300 digital accelerograms (270 of which belonging to RAN), with a very good signal-to-noise ratio, recorded by about 70 stations, installed on different site conditions at distances ranging from 0 to 300 km. The national and international relevance of this data set is enhanced by its contribution to filling gaps in the magnitude-distance distribution of worldwide strong motion records, especially for normal-fault earthquakes. Near-fault records were obtained by (i) an array of 6 stations installed by DPC in 2001 in the Aterno Valley to study seismic site effects; (ii) station AQK close to downtown L'Aquila; (iii) station AQU, belonging to the broad-band Mednet network, located in the L'Aquila historic castle; (iv) the stations of the INGV temporary network, installed in the epicentral region one day after the mainshock. These stations are located less than 5 km from the mainshock epicenter and are inside the surface projection of the fault rupture. This work presents an overview of the main features of seismic ground shaking during the L'Aquila sequence, referring to records of the mainshock and of the two strongest aftershocks. The dependence of the strong-motion parameters on distance, azimuth and site conditions as well as the characteristics of near-fault strong-motion records are discussed.

Keywords: L'Aquila earthquake, strong motion records, near fault.

1. Introduction

On April 6, 2009, at 1:32:40 GMT, a M_w 6.3 earthquake struck L'Aquila city, one of the largest urban centers in the Abruzzo region (central Italy) with about 70,000 inhabitants, causing about 300 deaths and vast destruction in the town and surrounding villages.

The earthquake occurred along a NW-SE trending normal fault, 15-18-km long, dipping about

45° SW. The hypocenter depth was estimated at 9.5 km, and the epicenter at less than 5 km SW of the town center (Chiarabba *et al*., 2009). The causative fault of the mainshock is associated with the tectonic depression of the Aterno River Valley, sited between two main calcareous ridges, the Velino – Sirente to the SW and the Gran Sasso to the N-NE. The maximum observed intensity is IX-X in the MCS scale and the most relevant damage is distributed in a NW-SE direction, with evident predominance towards SE (Galli and Camassi, 2009; Ameri *et al*., 2011).

According to regulations for the Italian territory, the area struck by the L'Aquila earthquake is classified as a zone characterized by a high level of seismic hazard (Gruppo di Lavoro MPS, 2004). In terms of probabilistic hazard assessment, the maximum peak ground acceleration (PGA) having a probability of 10% of being exceeded in 50 years is 255 cm/s^2.

This event represents the third largest earthquake recorded by strong-motion instruments in Italy, after the 1980, M_w 6.9, Irpinia and the 1976, M_w 6.4, Friuli earthquakes (Luzi *et al*., 2008).

The mainshock was followed, within the first week, by seven aftershocks with moment-magnitude greater than or equal to 5, the two strongest ones occurred on April 7 (M_w=5.6) and April 9 (M_w=5.4). The seismic sequence has been recorded by several digital stations of the Italian Strong-Motion Network (Rete Accelerometrica Nazionale, RAN), operated by the Italian Department of Civil Protection (DPC), by the Italian Seismometric Network (Rete Sismometrica Nazionale, operated by the institute INGV-CNT; http://cnt.rm.ingv.it), and by a temporary strong-motion array installed by the INGV MI-PV (http://www.mi.ingv.it). Presently, the ITalian ACcelerometric Archive (ITACA), the new Italian strong motion database (http://itaca.mi.ingv.it), includes more than 900 waveforms from the L'Aquila earthquake sequence, including the $M > 4$ aftershocks that occurred before April 13.

Strong motion data in near source regions were recorded by six accelerometric stations installed in 2001 by the DPC, across the upper Aterno Valley and by four INGV MI-PV temporary stations situated close to the villages mainly damaged during the mainshock. Although some of these stations either did not trigger or malfunctioned during the events, recordings from the array and the temporary network, together with the AQK and AQU stations located close to downtown L'Aquila, provide a near-fault, strong-motion data set never recorded to date in Italy for events with $M > 5$, and one of the few ones worldwide.

This work presents an overview of the main features of seismic ground motion during the L'Aquila sequence, referring to records of the mainshock and of the two strongest aftershocks. The dependence of the strong-motion parameters on distance, azimuth and site conditions is discussed, as well as the characteristics of near-fault strong motion records in terms of amplitude and frequency content.

2. Strong motion data set and site classification

In this work, we analyzed 136 recordings from strong-motion stations, extracted by the Italian Strong Motion Database ITACA triggered by the April 6, 2009, L'Aquila earthquake (hereinafter referred to as Event 1) and by the two largest aftershocks (2009/04/07 17:47:37, M_w 5.6 and 2009/04/09 00:52:59, M_w 5.4, hereinafter referred to as Event 2 and Event 3, respectively). Fig. 1 shows the location of the epicenters and of the closest recording stations, together with the focal mechanisms of the three events. Tables 1 and 2 list the source parameters of the events and the

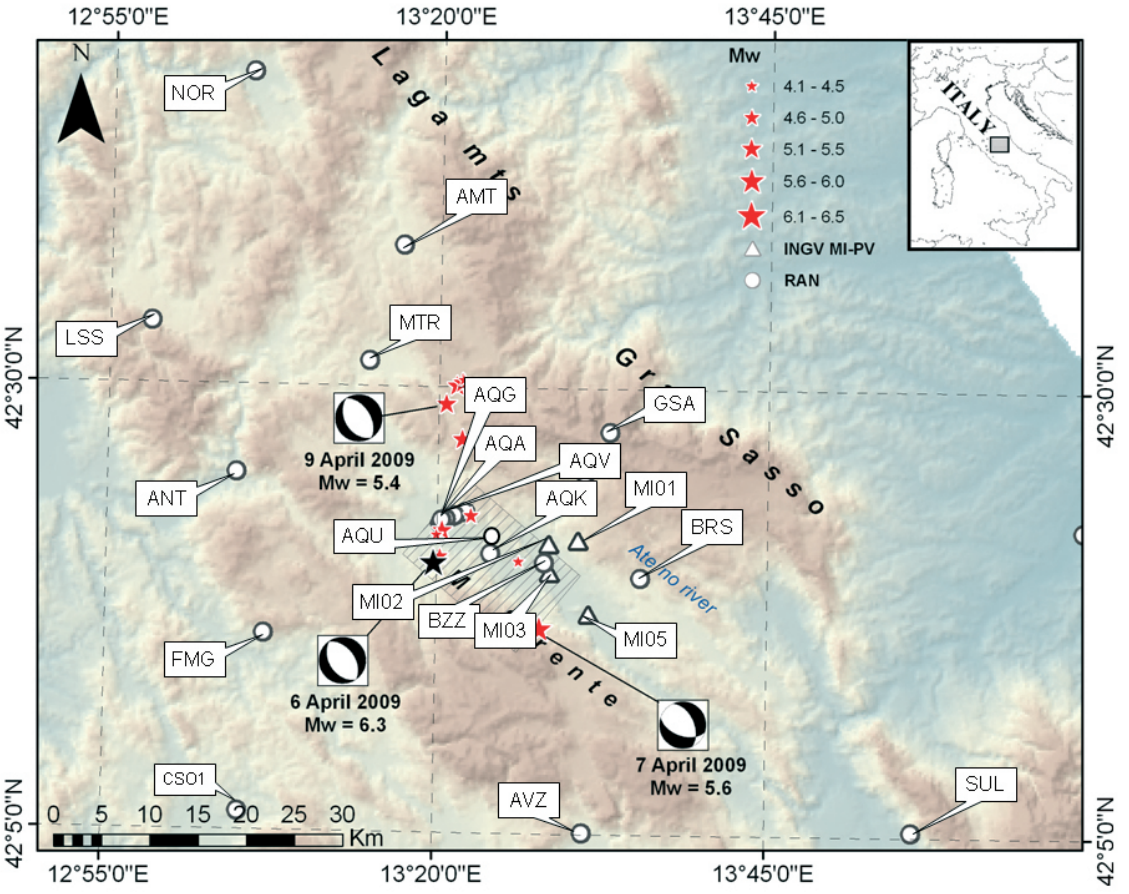

Fig. 1 - Location of the main events (M_w > 4) of the L'Aquila sequence (red stars) and of the accelerometric stations belonging to RAN (dots) and to INGV MI-PV (triangles). The surface projection of the fault is also shown (Falcucci *et al*., 2009). Focal mechanisms are shown for the three strongest events.

main information of the stations up to 100 km from the relative epicenters.

The RAN stations are equipped with three-component sensors set to 1 or 2 g full-scale, coupled with 24-bit digitizers with a sampling rate of 200 S/s. The accelerographs of the four INGV MI-PV temporary stations were equipped with both an accelerometer (Kinemetrics Episensor ES-T) and a seismometer (either Lennartz 3D-5s or 3DLite) connected to a Reftek130 6-channel digitizer with a sampling rate of 100 S/s.

The recorded waveforms were processed following the new ITACA procedure (Paolucci *et al*., 2011), which consists in: removal of the linear trend fitting the entire record; application of a cosine taper and of a 2nd order acausal time-domain Butterworth filter to acceleration time series; double integration to obtain displacement time series; linear de-trending of displacement; double-differentiation of displacement to get the corrected acceleration. Both the high-pass and low-pass filter corners were selected through visual inspection of the Fourier spectrum. The typical band-pass frequency range is between 0.1 and 25 to 40 Hz; the lower values of the high-cut off frequency have

Table 1 - Main source parameters of the considered events.

Date* yyyymmdd	time (UTC)* hhmmss	Lat.(N)* [°]	Lon.(E)* [°]	H* [km]	Ml*	Mw+	Strike+ [°]	Dip+ [°]	Rake+ [°]
20090406	013240	42.348	13.380	9.5	5.8	6.3	147.0 *133.0*	43.0 *54.0*	-88.0 *-102*
20090407	174737	42.275	13.464	15.1	5.3	5.6	109.0	51.0	-124.0
20090409	005259	42.484	13.343	15.4	5.1	5.4	148.0	40.0	-90.0

* from INGV-CNT Bulletin (Chiarabba *et al.,* 2009); + from Regional Centroid Moment Tensor (http://www.bo.ingv.it/RCMT/).
In italic: fault mechanism from Cirella *et al.* (2009), note that the reported rake angle corresponds to that associated to the maximum slip area on the fault.

been selected for the stations far away from the epicenter (epicentral distance, $R_{epi} > 100$ km).

The sites were classified according to Eurocode 8 [EC8: CEN (2004)] and the Italian Building Code (NTC08, 2008), based on the shear-wave velocity averaged over the top 30 m of the soil profile - V_{S30} (where EC8 class A: $V_{S30} > 800$ m/s, class B: $V_{S30} = 360$-800 m/s, class C: $V_{S30} = 180$-360 m/s, class D: $V_{S30} < 180$ m/s and class E: 5 to 20 m of C- or D-type alluvium underlain by stiffer material with $V_S > 800$ m/s). The class of each station has been attributed on the basis of a direct measure of V_{S30} or on geological/geophysical information (S4 project – http://esse4.mi.ingv.it – Deliverable D4, 2009).

The epicentral area corresponds to the upper and middle Aterno Valley, which is characterized by a complex tectonic evolution reflected by the high variability of the geological and geomorphologic patterns (Fig. 2a). The valley is superimposed on a Quaternary lacustrine basin of tectonic origin. The depth of the Quaternary deposits is variable, from about 60 m in the upper Aterno Valley to more than 200 m in the middle Aterno Valley (Bosi *et al*., 2003). L'Aquila lies on a fluvial terrace, some tens of meters thick, consisting of calcareous breccias and conglomerates with limestone boulders and clasts in a marly matrix. The terrace lies on the top of lacustrine sediments, mainly consisting of silty and sandy layers and minor gravel beds (De Luca *et al*., 2005). As shown in Fig. 2a, the terrace is at the left bank of the Aterno River Valley, which flows about 50 m below downtown L'Aquila.

Due to the complexity of the area, the ground motion is expected to be affected by local geological conditions. The site amplification effects for some of the strong motion stations considered have been recently spectrally investigated using strong motion recordings from 13 earthquakes of the L'Aquila seismic sequence with $M > 4.0$ (Bindi *et al*., 2009a). In particular, high-frequency amplifications were detected for sites in class B (e.g., Antrodoco, ANT), whereas amplification peaks at frequencies close to or smaller than 1 Hz are identified for class C.

The site responses at the stations belonging to the Aterno Valley array were also analyzed by Ameri *et al*. (2009) through the computation of the horizontal-to-vertical spectral ratios, HVSRs, (Lermo and Chavez-Garcia, 1993). Fig. 2b shows the average HVSR +/- one standard deviation as well as horizontal and vertical site responses estimated through the generalized inversion technique by Bindi *et al*. (2009a) for some stations of the Aterno Valley array and for AQK and AQU.

Table 2 – Strong-motion stations installed in the area that recorded at least one of the three strongest events. Geographical coordinates, site class according to EC8 site classification, and the event recorded at each station are reported in the relative column.

Name	Code	Owner	Lat. N(°)	Long. E(°)	EC8	#events
Antrodoco	ANT	DPC	42.4181	13.0786	A*	1 2 3
L'Aquila F. Aterno	AQA	DPC	42.3755	13.3393	B	1 3
L'Aquila Ferriera	AQF	DPC	42.3805	13.3547	B*	2
L'Aquila Colle Grilli	AQG	DPC	42.3735	13.3370	B	1 2 3
L'Aquila Aquilpark	AQK	DPC	42.3450	13.4009	B	1 2 3
L'Aquila Il Moro	AQM	DPC	42.3786	13.3493	A*	2 3
L'aquila Monte Pettino	AQP	DPC	42.3837	13.3686	A	2 3
L'Aquila Castello	AQU	Mednet	42.3539	13.4019	B*	1 2 3
L'Aquila Centro Valle	AQV	DPC	42.3772	13.3439	B	1 2 3
Assisi	ASS	DPC	43.0750	12.6041	A*	1 2
Avezzano	AVZ	DPC	42.0275	13.4259	B*	1 2 3
Barisciano	BRS	DPC	42.3239	13.5903	B*	3
Bazzano	BZZ	DPC	42.3370	13.4686	B	2 3
Castel di Sangro	CDS	DPC	41.7871	14.1119	A*	1 2 3
Chieti	CHT	DPC	42.3698	14.1478	B	1 2 3
Celano	CLN	DPC	42.0852	13.5207	A*	1 2 3
Carsoli	CSO1	DPC	42.1009	13.0881	A*	1 2 3
Cassino	CSS	DPC	41.4858	13.8231	A*	1 2 3
Cattolica	CTL	DPC	43.9550	12.7360	B*	1 2
Fiamignano	FMG	DPC	42.2680	13.1172	A*	1 2 3
Gran Sasso Assergi	GSA	DPC	42.4207	13.5194	C*	1 2 3
Isernia	ISR	DPC	41.6106	14.2359	C*	1 2
Leonessa	LSS	DPC	42.5582	12.9689	A*	1 2 3
Pescomaggiore	MI01	INGV-MI	42.3580	13.5098	A*	2 3
Paganica	MI02	INGV-MI	42.3545	13.4743	C*	2 3
Onna	MI03	INGV-MI	42.3274	13.4757	B	2 3
S. Eusanio Forc.	MI05	INGV-MI	42.2895	13.5253	B*	2 3
Mompeo	MMP	DPC	42.2486	12.7486	A*	1 2 3
Montereale	MTR	DPC	42.5240	13.2448	A*	1 2 3
Ortucchio	ORC	DPC	41.9536	13.6423	A*	1 2 3
Pescasseroli	PSC	DPC	41.8120	13.7892	A	2 3
Subiaco	SBC	DPC	41.9132	13.1055	A*	1 2
Scanno	SCN	DPC	41.9187	13.8724	A*	2 3
Spoleto cantina	SPC	DPC	42.7435	12.7397	C*	1 2 3
Spoleto	SPO	DPC	42.7336	12.7406	A*	1 2 3
Sulmona	SUL	DPC	42.0890	13.9340	A*	1 2 3

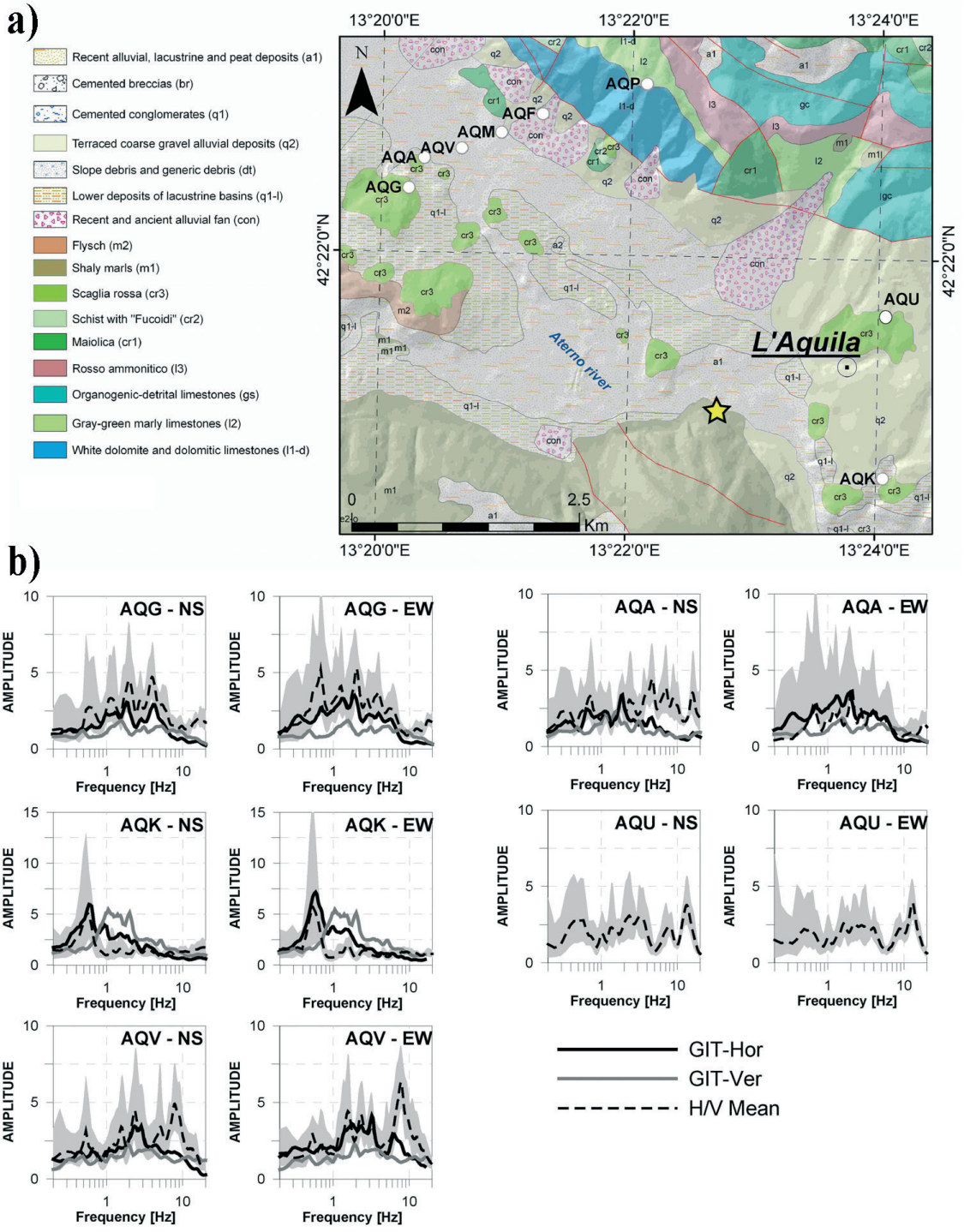

Fig. 2 – Upper panel: location of the strong motion stations of the Aterno Valley array and of AQK and AQU, plotted on local geology. The star indicates the mainshock epicenter. Lower panel: horizontal-to-vertical spectral ratios (HVSR), calculated at 5 stations (for both horizontal components) using the mainshock and 12 aftershocks of the L'Aquila seismic sequence, are shown as dashed lines (grey area indicates the ± 1 standard deviation). Empirical site response for horizontal (black line) and vertical (grey line) components estimated through generalized inversion technique by Bindi *et al*. (2009a) are also reported.

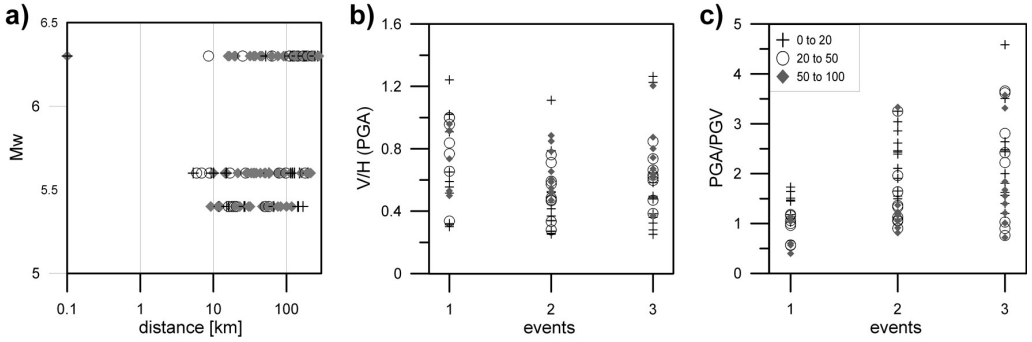

Fig. 3 - Magnitude – distance distribution of the strong-motion data recorded by the three strongest events of the L'Aquila seismic sequence (a). The data are grouped according to the EC8 classes (grey diamonds for class A, crosses for class B, circles for class C). Note that points with R_{JB}=0 are plotted at 0.1 km. Ratio between the vertical and horizontal (geometric mean) (PGA) for the 06-04-2009 Event 1, 07-04-2009 Event 2 and the 09-04-2009 Event 3 (b). Ratio between the horizontal (geometric mean) PGA and PGV (PGA/PGV) for the 06-04-2009 Event 1, 07-04-2009 Event 2 and the 09-04-2009 Event 3 (c).

In general, all sites are characterized by no-flat HVSRs: broadband amplification is found for rock sites (AQP, AQG) while the stations installed on Quaternary deposits of the upper Aterno Valley (AQA, AQV, AQK, AQU) show remarkable amplifications at specific frequencies. In particular, AQK, located in the centre of L'Aquila town has a strong amplification peak at low frequency (about 0.6 Hz), as also demonstrated by De Luca *et al*. (2005) using weak motion and ambient noise data. This peak is also observed at the AQU station but lower in amplitude.

3. Characteristics of the peak ground motions

The magnitude-distance distribution of the selected recordings is shown in Fig. 3a, grouping the data according to the site conditions. We used the Joyner-Boore distance (R_{JB}), which is the shortest horizontal distance from the surface projection of the fault rupture, for the main event, and the epicentral distance (R_{epi}) for the two aftershocks since we do not have precise information on the location and dimension of the fault rupture. Note that this is a common assumption in ground motion prediction equations (GMPEs) for magnitude smaller than about 5.5 (e.g., Akkar and Bommer, 2007; Bindi *et al*., 2009b).

The mainshock (Event 1) was recorded by 57 stations in the epicentral distances range from 1.7 km to about 276 km with R_{JB} ranging from 0 to 266 km. In particular, there are 9 records with epicentral distances less than 30 km and 5 records with R_{JB}=0. The largest PGA (PGV) is 646 cm/s^2 (43 cm/s) recorded at station AQV; in general, all PGAs recorded at an epicentral distance of less than 5 km are greater than 350 cm/s^2 and the PGVs greater than 30 cm/s.

The two strongest aftershocks (Event 2 and Event 3), M_w=5.6 and M_w=5.4, were recorded by 44 and 35 stations respectively, with most of them located at epicentral distances of less than 60 km. In particular, Event 2 and Event 3 were recorded by 12 and 9 stations within 16 km from the epicenter, respectively.

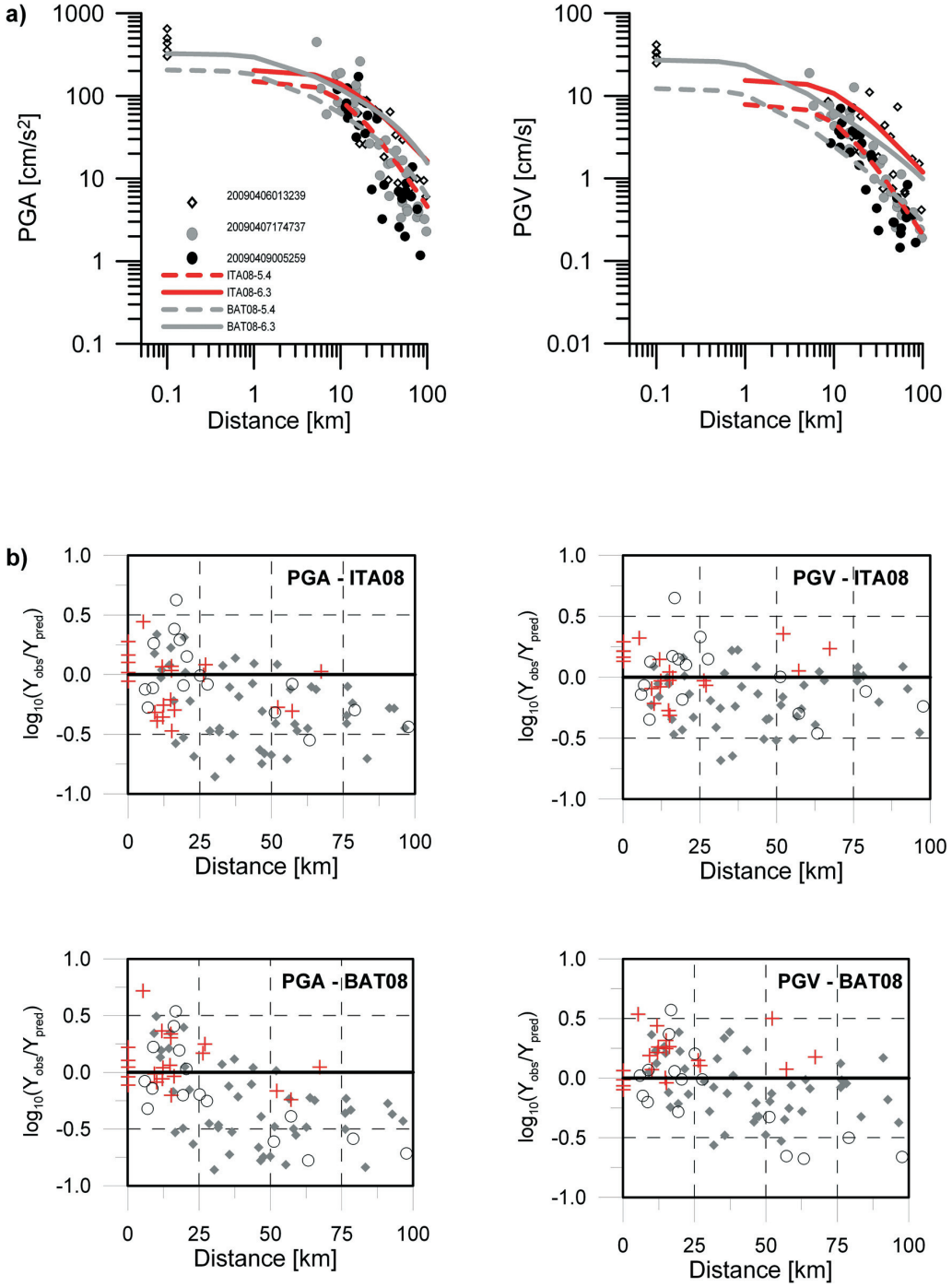

Fig. 4 - Maximum horizontal PGA (left) and PGV (right) versus distance up to 100 km (a). The red and grey lines show the predictions computed by the Italian and global empirical GMPEs [ITA08=Bindi *et al*. (2009b); BAT08=Boore and Atkinson (2008)] for rock sites and magnitude M_w 6.3 and 5.4. Observed peak values are indicated with diamonds for Event 1 (06-04-2009), grey circles for Event 2 (07-04-2009) and black circles for Event 3 (09-04-2009) Residuals versus distance for PGA (right) and PGV (left): the residuals are computed using the ITA08 (top) and the BAT08 (bottom) predictions (b). An equivalent EC8 class is used for the GMPEs. For ITA08 class 0 corresponds to A (red crosses), class 1 to B (grey diamonds) and class 2 to C (circles). For BAT08 model, V_{S30} = 900 m/s is assigned for class A; V_{S30} =537 m/s for class B and V_{S30} = 255 m/s for class C.

Table 3 – PGA/PGV [g/m/s] values (mean ± standard deviation) calculated for the three events and grouping the data according to distance ranges or different site classifications.

	Event 1 [g/m/s]	**Event 2 [g/m/s]**	**Event 3 [g/m/s]**
All	0.71±0.40	1.48±0.80	1.90±1.05
< 20 km	1.37±0.24	2.16±0.67	2.30±0.92
>20 km	0.58±0.27	1.17±0.80	1.65±1.07
EC8 A	0.77±0.40	1.56±0.88	1.92±1.16
EC8 B	0.61±0.37	1.37±0.82	1.58±0.94
EC8 C	0.73±0.48	1.43±0.56	2.39±0.83

The maximum PGA and PGV from Event 2 are 674 cm/s^2 and 23.5 cm/s, respectively, recorded at the closest station MI05, situated at 5.3 km from the epicenter. The maximum recorded PGA and PGV from Event 3 are 177.6 cm/s^2 and 8.2 cm/s, respectively, recorded by the GSA station at the epicentral distance of 16 km.

Fig. 3b shows the vertical-to-horizontal (V/H) PGA ratio (considering the geometric mean of the horizontal components) for the three events, grouping the peak values according to the distance. Values typically range between 0.25 and 0.75, and the rule-of-thumb of a 2/3 ratio between vertical and horizontal PGA is, on average, satisfied. The observed ratios at stations with $R_{JB} = 0$ are larger than 1 confirming that, in the near-source region, the vertical ground motions may be of the same order or significantly exceed the horizontal ones (see e.g., Bozorgnia and Campbell, 2004). It is also worth noting that the ratio of V/H ground motion amplitude may also depend on site conditions. For example, V/H ratio is larger than 0.8 at some stations (i.e., BRS and AVZ, both classified as class B) farther than 20 km from epicenters, that are known to be affected by amplification of the vertical component (Bindi *et al*., 2009a).

A very simple characterization of the ground motions from the three events can be obtained computing the PGA-to-PGV ratio: low values signify records with low predominant frequencies, broader response spectra and longer duration (Kwon and Elnashai, 2006). Fig. 3c shows the PGA-to-PGV ratio (geometric mean of horizontal components) for the three events computed considering stations at distance less than 100 km. As expected, the two weaker events have similar distributions, while the mainshock records are characterized by higher, low-frequency energy. The mean PGA-to-PGV ratio (Table 3), computed for the recordings of the entire data set are (0.71±0.4) g/ms^{-1} for Event 1, (1.48±0.8) g/ms^{-1} for Event 2 and (1.9±1.1) g/ms^{-1} for Event 3. Following the classification by Zhu *et al*. (1988) and Kwon and Elnashai (2006), the main shock can be classified as a High Velocity-Low Acceleration earthquake (HV-LA: PGA-to-PGV< 0.8g/m s^{-1}). Interestingly, these ratios assume the lowest values when large distance records are included (i.e., > 20 km), while the PGA-to-PGV ratios of the near-source recordings are about 1. The same trend is observed for the two aftershocks.

In Fig. 4a, the observed PGAs and PGVs (maximum between the horizontal components) for the three events are plotted as a function of distance and compared with those estimated from national [ITA08=Bindi *et al*. (2009b)] and global [BAT08=Boore and Atkinson (2008)] empirical

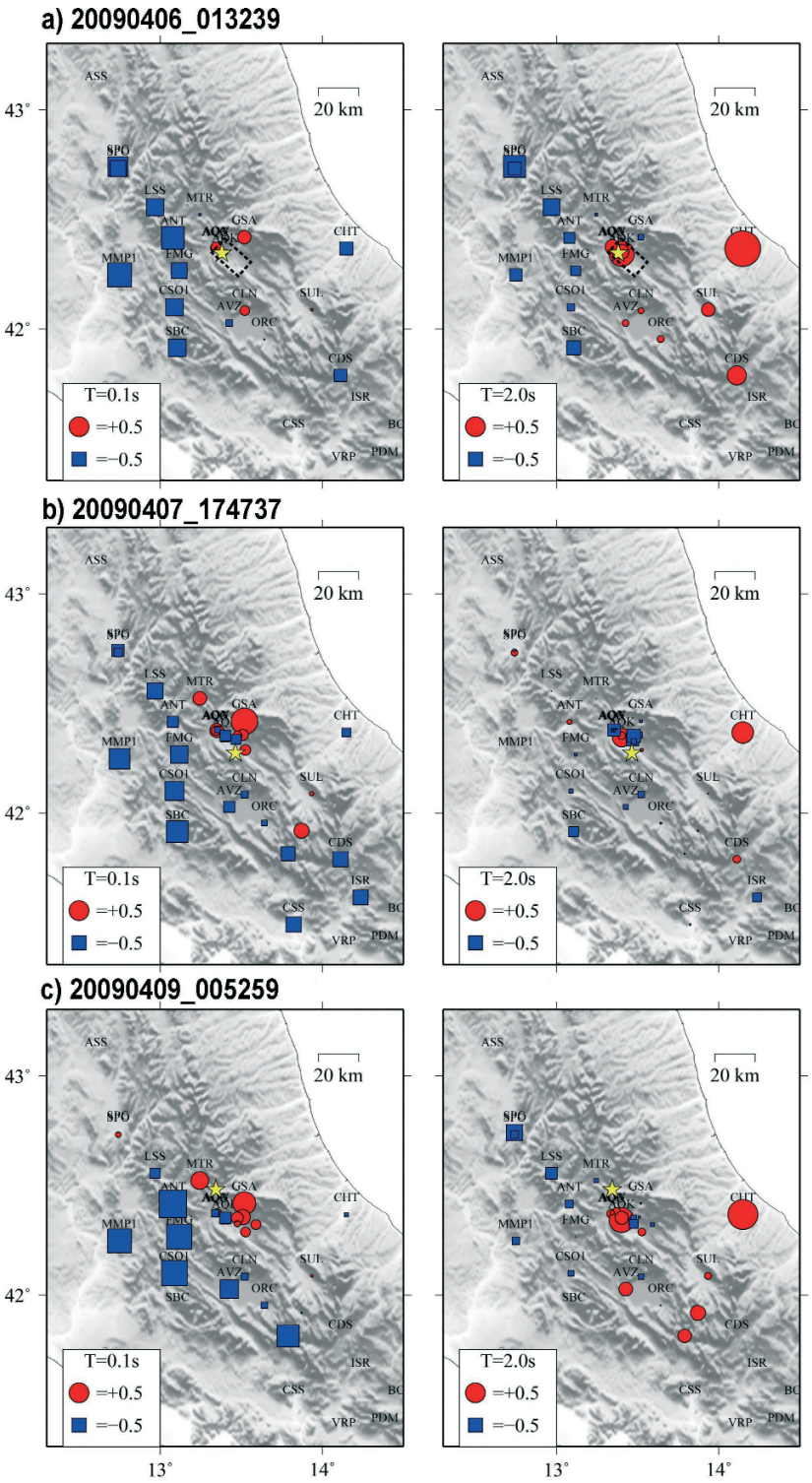

Fig. 5 - Spatial distribution of the residuals. For each site, residuals are calculated as log10(observed/predicted) where the Italian empirical GMPE [ITA08=Bindi *et al*. (2009b)] is used for each specific site class. Red circles indicate underestimation, while blue squares indicate overestimation. The residuals are computed for the maximum SA at 0.1 s (left) and 2 s (right) for Event 1 (a) Event 2 (b) and Event 3 (c).

GMPEs, and used here as references (Fig. 4a). Formally, the BAT08 equation is developed for an orientation-independent measure of ground motion. We used the relationships proposed by Beyer and Bommer (2006) to convert the BAT08 median estimates to the maximum horizontal component of motion for consistency with the other GMPEs.

On average and especially for the two aftershocks, the PGVs are fitted by the empirical curves while the PGAs decay faster (particularly at distances larger than 20 km). The peak ground motions for the main event show a more complex trend: observed PGA and PGV at short distances agree with BAT08 and exceed the ITA08 predictions, as this GMPE is based on a data set that poorly samples the near-fault distances. At larger distances, the observed data are scattered with some of the data following the median trend of the GMPEs (computed for M_w= 6.3), while others seem to better agree with the median curve for M_w = 5.4. This feature has been previously recognized by other authors (Ameri *at al.,* 2009), showing that the L'Aquila mainshock ground motion is strongly azimuthally dependent. In particular, these authors found that, for distances from 10 to about 100 km and for all site classes, the data east of the epicenter (roughly azimuths form 0° to 180°) follow the median trend estimated by the GMPEs, while the sites located in the western sector (180° to 360°) are less than the median minus one standard deviation. They also suggested that this asymmetry in attenuation of PGA may be both ascribed to source and path effects.

To better understand the attenuation of ground motion in the L'Aquila region, the residuals, defined as the logarithm difference between observations and predictions, are plotted as a function of distance, grouping the data for site classes (Fig. 4b). The observed PGAs for the three site classes are constantly lower than the predicted values for distance larger than 25 km, especially in the case of the global attenuation model. On the other hand, residuals for PGV are between +/- 0.5 and no dependence on distance and site condition is observed. These results suggest that the high-frequency ground motions in the L'Aquila region decay faster with respect to the average trends described by national and global GMPEs.

4. Spatial distribution of ground motion

An overview of the spatial variability of ground motion recorded in the epicentral area during the April 6 earthquake and the two aftershocks is illustrated in Fig. 5, where the distributions of the residuals between observed and predicted acceleration response spectra (5% damping) are plotted. To compute the residuals, the empirical GMPE developed for the Italian territory is adopted [ITA08=Bindi *et al*. (2009b)] at periods of 0.1 s and 2 s, considering appropriate site classes and distances of up to 100 km from the epicenters.

For the mainshock (Fig. 5a), the positive residuals (observations larger than predictions) are mainly localized SE of the epicenter, especially for long-period motions. Conversely, negative residuals are found at short and long periods in the north-western area. Clear trends in the high-frequency residuals are found also in case of Event 2 and Event 3. For both, an evident underestimation of the observed spectral ordinates at T = 0.1 s appears in the western sector (i.e., toward the Tyrrhenian Sea), whereas overestimation is observed in the opposite sector (i.e., Adriatic Sea). At long periods, for Event 2, the absolute values of residuals are, in general, lower than 0.5 except for some sites in the Aterno Valley. On the other hand, for Event 3, the regional

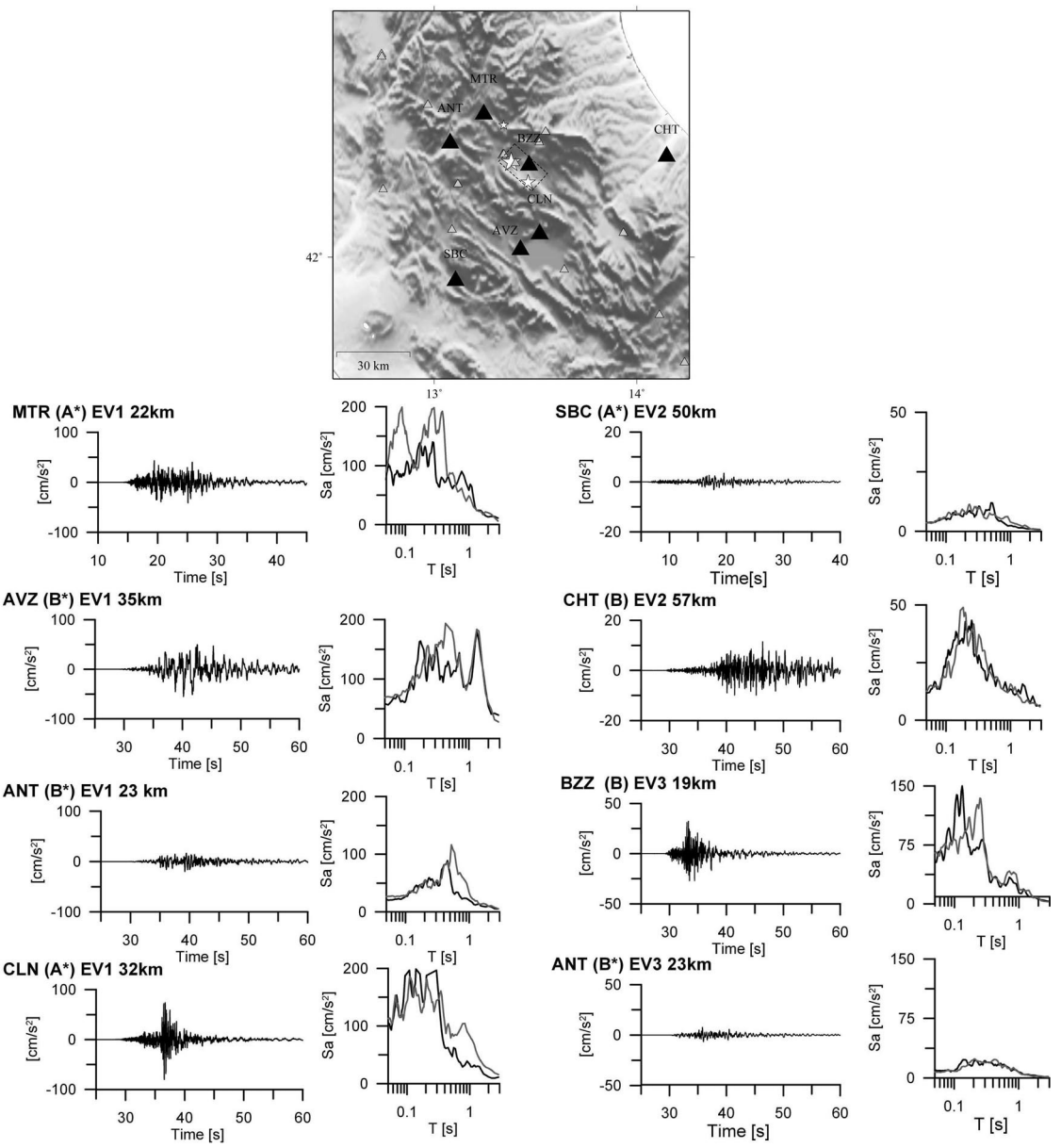

Fig. 6 – Examples of acceleration time series in cm/s^2 (E-W component) and acceleration response spectra (EW component: black; N-S component: grey) recorded during Event 1, Event 2 and Event 3 by some selected stations in the epicentral area (black triangles). The white stars indicate the location of the epicenters. Stations are located in the distance range from 18 to 60 km at different azimuths with respect to the epicenters. For each station, the identification code, the site class, the recorded event and the epicentral distance are reported.

distribution of the long-period residuals is characterized by an asymmetric shape, with a clear underestimation area (i.e., positive residuals) elongated in the SE direction with respect to the epicenter. For the three earthquakes, the highest positive long-period residuals always occurred at AQK and CHT stations, both affected by strong site amplification at low frequency (< 1 Hz).

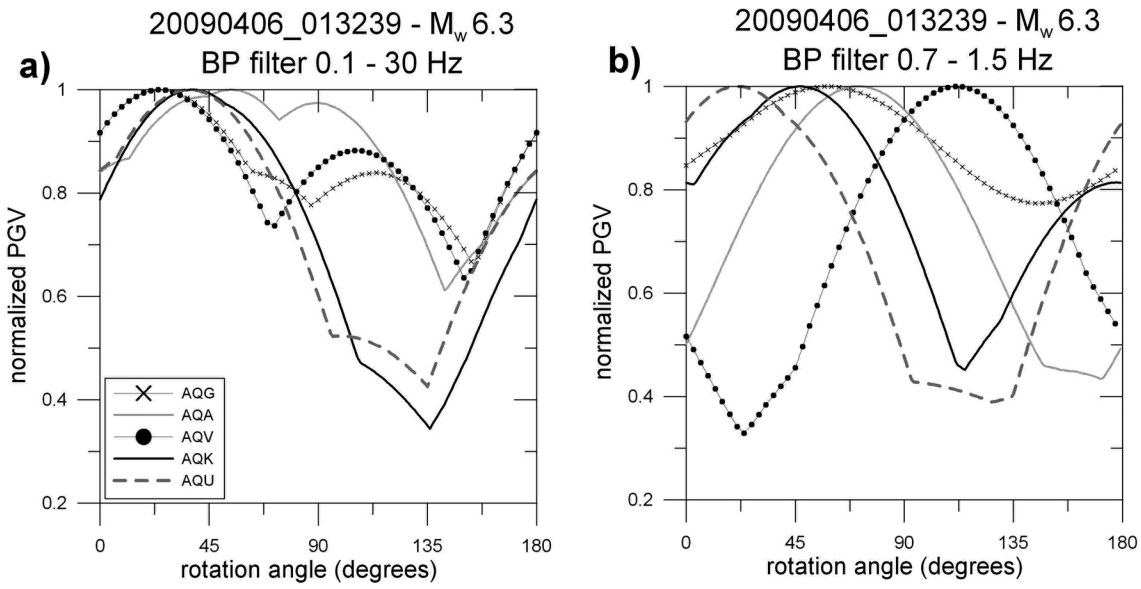

Fig. 7 - Normalized PGV as a function of the rotation angle for the five near-source mainshock recordings, considering 0.1-30 Hz (a) and 0.7-1.5 Hz (b) band-pass filtered time series. 0° and 90° represent the N-S and E-W direction (as-recorded PGVs). The vertical dashed lines are the SN direction (44°) and SP direction (133°) according to the fault rupture model proposed by Cirella *et al*. (2009).

The asymmetric regional distribution of residuals can be ascribed both to source and path effects. Directivity effects due to the rupture propagation over the fault can cause large variability of ground motion due to the amplification in the direction toward which the rupture propagates (forward directivity) and de-amplification in the opposite direction (backward directivity) (e.g., Somerville *et al*., 1997). On the other hand, different seismic wave attenuation properties of the Earth's crust can also be responsible for the azimuthal variability of residuals. Indeed, the different attenuation between the eastern and western Apennine sectors has been observed (Mele *et al*., 1997). Evident forward and backward directivity effects have been recognized for the mainshock through the analysis of the instrumental and macroseismic data (Cirella *et al*., 2009; Pino and Di Luccio, 2009; Akinci *et al*., 2010; Ameri *et al.,* 2011), caused by the fast quasi-unilateral rupture propagation towards a SE direction along the seismogenic fault. Propagation properties and seismic wave attenuation at regional scale should be investigated in order to explain the difference between the distribution of the short period residuals in the western region with respect to the eastern one.

The large variability of ground motion in the epicentral area is highlighted when recordings at stations, located at comparable distances from the epicenter but at different azimuths, are compared (Fig. 6). The accelerogram (E-W component) of the mainshock recorded at the ANT station, to the west of the epicenter, shows lower amplitudes than that at the eastern CLN station. Furthermore, larger amplitudes are found southwards, as shown by the AVZ and MTR recordings, placed in opposite directions with respect to the epicenter. Also the strong-motion data recorded during Events 2 and 3 show differences in amplitude depending on their azimuths. Examples are

the recordings at CHT and SBC stations located at an epicentral distance of about 50 km, but in the eastern and western sectors, respectively, and, for Event 3, the BZZ and ANT recordings at sites placed SE or NW of the epicenter. Site effects also play an important role in defining some characteristics of the ground motion. An example is the large spectral ordinate at T = 1.5 s of the acceleration response spectra observed at AVZ, installed close to the edge of the Fucino Basin.

5. Characteristics of near-source records

The stations of the Aterno array (Fig. 2) are located within the surface projection of the L'Aquila mainshock fault and are at distances of less than 5 km from the mainshock epicenter (Fig. 1) and provide, together with the AQK and AQU stations, high quality near-fault strong-motion recordings.

Ameri *et al*. (2009) showed that velocity pulses are present at the beginning of all records and to a larger extent on AQK. Such pulses are due to the rupture propagation toward the sites at a velocity that is close to that of the shear-waves causing most of the seismic radiation from the fault to arrive compressed in time (Somerville *et al*., 1997). The radiation pattern of the shear dislocation on the fault causes this large pulse of motion to be oriented in the direction perpendicular to the fault, resulting in larger ground motions in the strike-normal (SN) direction than in the strike-parallel (SP) direction at periods longer than about 0.5 s (Somerville, 2003; Bray and Rodriguez-Marek, 2004). In the case of dip slip faults (as for the L'Aquila mainshock fault), near-source directivity pulses are expected for sites located above the fault, in the up-dip direction and close to the surface termination of the fault. Previous studies showed that the use of PGV is adequate as the representation of the amplitude of the velocity pulse in the time domain (Mavroeidis and Papageorgiou, 2003; Brady and Rodriguez-Marek, 2004) and larger PGV are typically observed in the SN direction.

We investigated the PGV of the AQA, AQV, AQG, AQK and AQU corrected records as a function of sensor orientation, in order to indentify the direction of maximum amplitude of the velocity pulses. Fig. 7a shows the normalized PGVs obtained by rotating the N-S time series over all non-redundant rotation angles. Several comments can be made. First, there is a substantial variation in PGV with respect to the as-recorded values, represented by 0° and 90° rotation angles. For instance, the PGV in the E-W direction recorded at the AQU station is about 60% of the maximum horizontal PGV. As we do not know what will be the source-to-sensor azimuth for future earthquakes, we have to be aware that the near-fault ground motions recorded in the standard directions (i.e., N-S and E-W) can be substantially different to that of other horizontal directions. To account for this limitation, recently, orientation-independent, ground-motion intensity measures have been proposed in the context of GMPEs (Boore *et al*., 2006). Secondly, the direction of the maximum PGV coincides surprisingly well, for all sites, with the SN direction (43°) when a fault strike of 133° is considered [as reported by Cirella *et al*. (2009)]. On the other hand the direction of minimum PGV coincides, as expected, with the SP direction (Somerville *et al*., 1997). Note that this feature is more evident for AQK and AQU records. Third, there are systematic differences between the three stations of the Aterno-Valley array (AQG, AQA and AQV) and the two stations located at the L'Aquila city (AQK and AQU). The latter two present a clear maximum PGV in the SN direction and a minimum in the SP direction, which is 60-70%

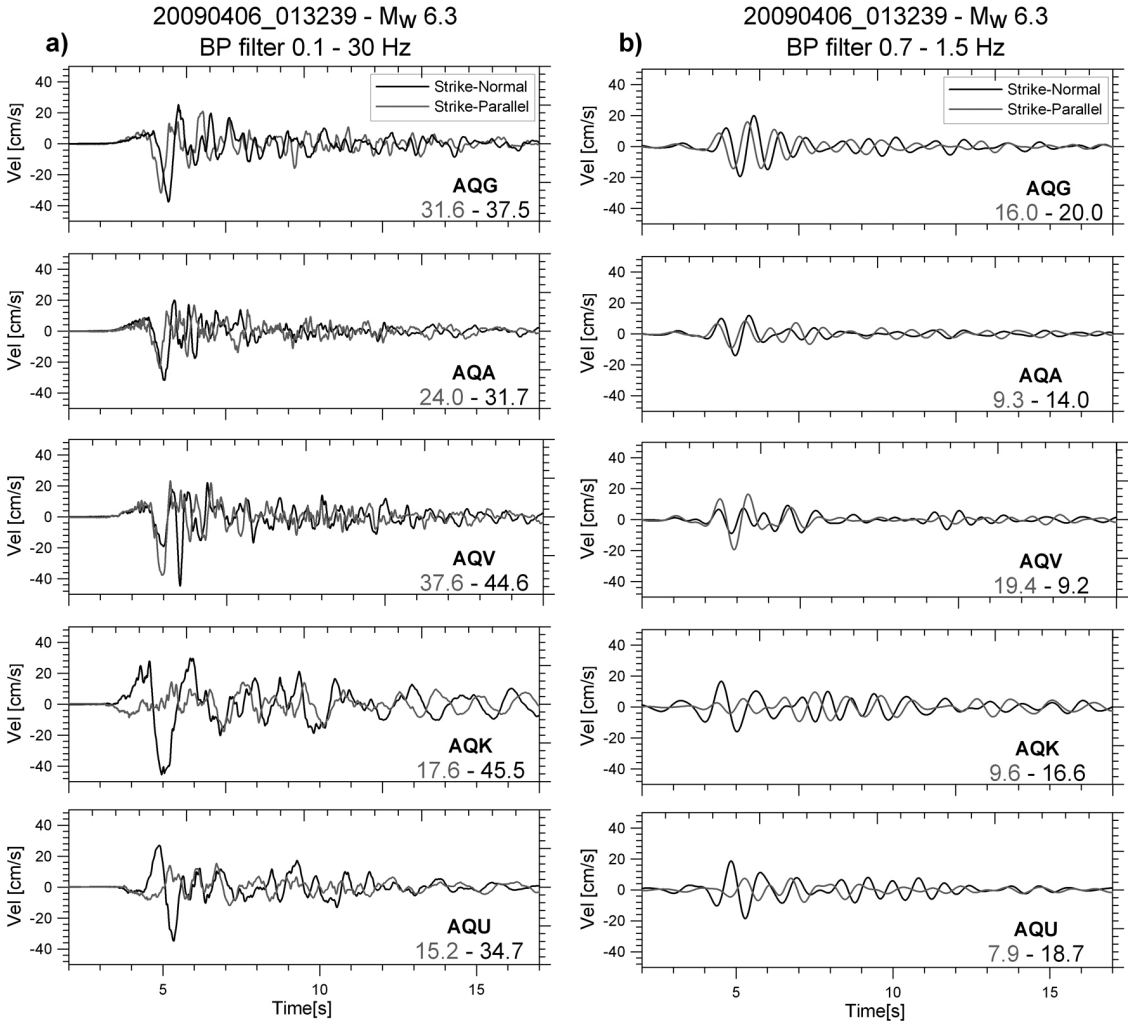

Fig. 8 - SN (black) and SP (gray) velocity time series at the five near-source stations, considering 0.1-30 Hz (a) and 0.7-1.5 Hz (b) band-pass filters. The labels report the PGV in the two directions (cm/s).

smaller than the maximum value. For the other three stations, a local maximum is visible at about 90°-110°.

In order to investigate whether such differences are due to different site amplification effects at the array stations, we filtered the records with a band-pass filter between 0.7 and 1.5 Hz and calculated the PGVs from rotated time series (Fig. 7b). The choice of cut-off frequencies aims at emphasizing the source-related pulses and to minimize the effects of local site conditions. The site effects at the three Aterno array stations show, in general, amplification peaks at frequencies higher than 1-2 Hz, whereas AQK and AQU stations are characterized by amplification peaks at about 0.6 Hz. [see Fig. 2 and Ameri *et al*. (2009) and Bindi *et al*. (2009a)]. On the other hand, the pulses period is generally recognized to be around 1 s, at least in the SN direction (Chioccarelli

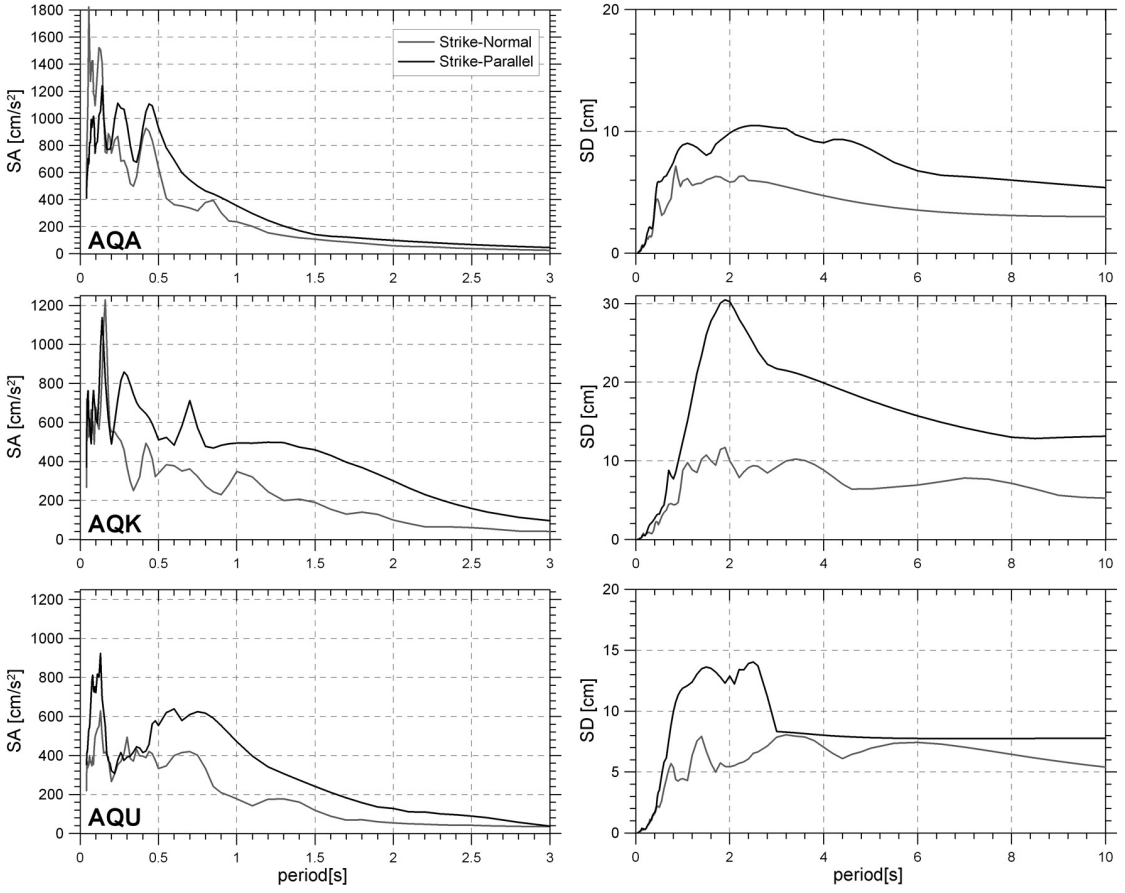

Fig. 9 - Comparison of 5% damped acceleration (SA, left) and displacement (SD, right) response spectra along the SN (black) and SP (gray) components.

and Iervolino, 2010; Paolucci and Smerzini, 2010).

Fig. 7b shows that for AQK and AQU records the direction of maximum and minimum PGVs are still in good agreement with the SN and SP directions, respectively (though small deviations are observed for the maximum PGV of AQU and the minimum of AQK). On the other hand AQG, AQA and AQV stations show a different distribution of PGV as a function of the rotation angle with respect to what can be observed in Fig. 7a and the local maximum/minimum PGVs disappear. In particular, the AQV record presents the maximum and minimum PGVs close to the SP and SN direction, respectively, conversely to what can be observed for the other records. As the AQV station is located at the center of the Aterno Valley, there is the suspicion that directionality in site amplification might influence the direction of maximum PGV presented in Fig. 7b.

Fig. 8 shows the velocity time series, recorded at the five near-source stations, rotated in the SN (43°) and SP (133°) directions for both 0.1-30 Hz (Fig. 8a) and 0.7-1.5 Hz (Fig. 8b) band-

pass filters. For AQG, AQA and AQV stations, pulses are visible at the beginning of the records in both SN and SP directions, and the PGVs are comparable in the two directions (though the SN PGV is still to some extent larger). On the contrary, for AQK and AQU, pulses are clearly visible only on the SN directions, whereas the amplitude of the SP time series is substantially smaller.

The very large amplitude of the pulse in the SN direction of the AQK record, compared to AQU, is most likely a result of a complex coupling of the source mechanism and the deep structure of the Aterno basin, where the lacustrine sediments reach around a 250 m depth right underneath L'Aquila, as previously mentioned. This is confirmed by the filtered time series (Fig. 8b), that shows almost identical SN pulses for both AQK and AQU stations.

It is interesting to note that the SN PGV for AQV the record is not given by the first pulse in the time series (that is larger in the SP direction), but by a second pulse, with a shorter period, visible only in the SN direction. Such second pulse disappears when filtered time series are considered (Fig. 8b), leading to a large velocity pulse in the SP direction, according to what can be observed in Fig. 7b.

Pulse-type records are of great interest to structural engineering because the seismic action is expected to be peculiar with respect to ordinary records. Indeed, the elastic demand of pulse-like signals is generally larger than that of ordinary recordings, particularly concerning the SN direction. Moreover, the spectral shape is non-standard with an increment of spectral ordinates in the range around the pulse period and, because the pulse period is generally at low frequencies (comparable to the fundamental period of most of the common structures), the inelastic demand can be particularly high and develop in a comparatively short time (Tothong and Luco, 2007; Chioccarelli and Iervolino, 2010).

In Fig. 9, the elastic SA and spectral displacement (SD), at 5% damping, are presented for SN and SP components of AQA, AQK and AQU records. The SA demand at a short period (< T= 0.2 s) is similar for both SN and SP motions, whereas at longer periods the spectral ordinates are systematically higher in the SN directions. This is particularly evident when looking at SD where the SN ordinates are remarkably larger than the SP ones.

6. Conclusions

The April 6, 2009 L'Aquila M_w 6.3 earthquake and its aftershocks yielded the most extensive set of digital strong-motion data, in particular in the near-source region, ever obtained in Italy. The mainshock and the two following largest events provide more than 130 three-component, strong-motion records, with about 90 records within 100 km of the corresponding epicenters.

The analysis of the observed peak ground motion and their ratios (V/H and PGA/PGV) allows us to highlight some important features on the recorded ground motion in the epicentral area.

A faster decay with distance of the high-frequency with respect to the low-frequency radiation is observed, leading to the classifiction of the Abruzzo earthquake as a High Velocity-Low Acceleration event. The residuals of spectral ordinates at 0.1 s and 2 s, computed with respect to empirical predictions show a clear dependence on azimuth, that can be attributed both to source effects (i.e., directivity effects) and to different attenuation properties of seismic waves at crustal scale. In particular, for the three events, a clear underestimation of the short-period ground motion appears west of the Apennine chain, whereas the overestimation is observed in the

opposite sector (i.e., towards the Adriatic Sea), in agreement with the different shear-wave attenuations reported for the two zones in literature (e.g., Mele *et al*., 1997). Site effects also play an important role in explaining the observed ground motion variability.

The analyses of mainshock near-fault records show that peak motion varies significantly for stations within 5 km from the epicentre, spanning from the 0.66 g, recorded at AQV, to 0.26 g at AQU. All these recordings are characterized by near-source velocity pulses with periods around $T = 1$ s, having maximum amplitude oriented in the direction perpendicular to the fault strike.

However, there are systematic differences in the SN and SP velocities between the three stations of the Aterno-Valley array (AQG, AQA and AQV) and the two stations located at L'Aquila city (AQK and AQU). In the former, velocity pulses of comparable amplitude are visible in both SN and SP directions, while, in the latter they are clearly visible only in the SN direction. This study suggests that their amplitude and orientation, in the case of the array sites, is influenced also by the Aterno Valley site effects.

Finally, we emphasize that because of the near-fault conditions, the complex geological setting and the availability of several good-quality near-fault records, this earthquake resulted in an important benchmark that provided an impressive and instructive picture of strong ground motion in the epicentral region of a normal fault earthquake.

Acknowledgements. This work has been partly supported by the Italian Department of Civil Protection under Project S4, Italian strong-motion database, within the DPC-INGV 2007-09 agreement. The pertinent comments and suggestions of Aldo Zollo and an anonymous reviewer helped to improve the quality of the paper.

REFERENCES

Akkar S. and Bommer J.J.; 2007: *Prediction of elastic displacement response spectra in Europe and the Middle East.* Earthquake Eng. Struct. Dyn., **36**, 1275-1301.

Akinci A., Malagnini L. and Sabetta F.; 2010: *Characteristics of the strong ground motions from the 6 April 2009 L'Aquila earthquake, Italy*. Soil Dyn. Earthquake Eng, **30,** 320-335.

Ameri G., Bindi D., Pacor F. and Galadini F.; 2011: *The 6 April 2009, M_w 6.3, L'Aquila (Central Italy) earthquake: directivity effects on intensity data.* Geoph. J. Int., DOI: 10.1111/J.1365-246x.2011.05o69.x

Ameri G., Massa M., Bindi D., D'Alema E., Gorini A., Luzi L., Marzorati S., Pacor F., Paolucci R., Puglia R. and Smerzini C.; 2009: *The 6 April 2009, M_w 6.3, L'Aquila (Central Italy) earthquake: strong-motion observations.* Seismol. Res. Lett., **80**, 951-966.

Beyer K. and Bommer J.J.; 2006: *Relationships between median values and between aleatory variabilities for different definitions of the horizontal component of motion.* Bull. Seism. Soc Am., **96**, 1512-1522.

Bindi D., Pacor F., Luzi L. Massa M. and Ameri G.; 2009a: *The M_w 6.3, 2009 L'Aquila earthquake: source, path and site effects from spectral analysis of strong motion data.* Geoph. J. Int., **179**, 1573–1579.

Bindi D., Luzi L. , Massa M. and Pacor F.; 2009b: *Horizontal and vertical ground motion prediction equations derived from the Italian Accelerometric Archive (ITACA)*. Bull. Earthquake Eng., doi:10.1007/s10518-009-9130-9.

Boore D.M. and Atkinson G.M.; 2008: *Ground-motion prediction equations for the average horizontal component of PGA, PGV, and 5%-damped PSA at spectral periods between 0.01s and 10.0s.* Earthquake Spectra, **24**, 99-138.

Boore D., Watson-Lamprey M.J. and Abrahamson N.A.; 2006: *GMRotD and GMRotI: Orientation-independent measures of ground motion.* Bull. Seism. Soc. Am., **96**, 1502–1511.

Bosi C., Galadini F., Giaccio B., Messina P. and Sposato A.; 2003: *Plio-Quaternary continental deposits in the Latium-Abruzzi Apennines: the correlation of geological events across different intermontane basins.* Il Quaternario, **16**,

55-76.

Bozorgnia Y. and Campbell K.W.; 2004: *The vertical to horizontal response spectral ratio and tentative procedures for developing simplified V/H and vertical design spectra.* J. Earth. Eng., **8**, 175-207.

Bray J.D. and Rodriguez-Marek A.; 2004: *Characterization of forward-directivity ground motions in the near-fault region.* Soil Dynam. Earthquake Eng., **24**, 815–828.

CEN Comité Européen de Normalisation; 2004 : *Eurocode 8: design of structures for earthquake resistance—Part 1: general rules, seismic actions and rules for buildings.* Brussels: Comité Européen de Normalisation.

Chiarabba C., Amato A., Anselmi M., Baccheschi P., Bianchi I., Cattaneo M., Cecere G., Chiaraluce L., Ciaccio M.G., De Gori P., De Luca G., Di Bona M., Di Stefano R., Faenza L., Govoni A., Improta L., Lucente F.P., Marchetti A., Margheriti L., Mele F., Michelini A., Monachesi G., Moretti M., Pastori M., Piana Agostinetti N., Piccinini D., Roselli P., Seccia D. and Valoroso L.; 2009*: The 2009 L'Aquila (central Italy) M_W 6.3 earthquake: main shock and aftershocks*. Geophys. Res. Lett., **36**, L18308, doi: 10.1029/2009GL039627.

Chioccarelli E. and Iervolino I.; 2010: *Near-source seismic demand and pulse-like records: a discussion for L'Aquila earthquake.* Earthquake Eng. Struct. Dyn., doi: 10.1002/eqe.987.

Cirella A., Piatanesi A., Cocco M., Tinti E., Scognamiglio L., Michelini A., Lomax A. and Boschi E.; 2009: *Rupture history of the 2009 L'Aquila (Italy) earthquake from non-linear joint inversion of strong motion and GPS data.* Geoph. Res. Lett., **36**, L19304.

De Luca G., Marcucci S., Milana G. and Sanò T.; 2005: *Evidence of low-frequency amplification in the city of L'Aquila, central Italy, through a multidisciplinary approach.* Bull. Seism. Soc. Am., **95**, 1469-1481.

Falcucci E., Gori S., Peronace E., Fubelli G., Moro M., Saroli M., Giaccio B., Messina P., Naso G., Scardia G., Sposato A., Voltaggio M., Galli P. and Galadini F.; 2009: *The Paganica fault and surface coseismic ruptures caused by the 6 April 2009 earthquake (L'Aquila, central Italy).* Seismol. Res. Lett., **80**, 940–950.

Galli P. and Camassi R. (eds); 2009: *Rapporto sugli effetti del terremoto aquilano del 6 aprile 2009.* Rapporto congiunto DPC-INGV, 12 pp. Available at: http://portale.ingv.it/real-time-monitoring/quest/aquilano-06-04-2009/).

Gruppo di Lavoro MPS; 2004: *Redazione della mappa di pericolosità sismica prevista dall'Ordinanza PCM del 20 marzo 2003.* Rapporto Conclusivo per il Dipartimento della Protezione Civile, INGV, Milano-Roma, 65 pp. + 5 appendici. In Italian.

Kwon O.S. and Elnashai A.; 2006: *The effect of material and ground motion uncertainty on the seismic vulnerability curves of RC structure.* Eng. Struct., **28**, 289–303.

Lermo J. and Chavez-Garcia F.; 1993: *Site effect evaluation using spectral ratio with only one station.* Bull. Seism. Soc. Am., **83**, 1574-1594.

Luzi L., Hailemikael S., Bindi D., Pacor F., Mele F. and Sabetta F.; 2008: *ITACA (ITalian Accelerometric Archive): a web portal for the dissemination of Italian strong-motion data.* Seismol. Res. Lett., **79**, 716-722.

Mavroeidis G.P., and Papageorgiou A.S.; 2003: *A mathematical representation of near-fault ground motions.* Bull. Seism. Soc. Am., **93**, 1099–1131.

Mele G., Rovelli A., Seber G. and Barazangi M.; 1997: *Shear wave attenuation in the lithosphere beneath Italy and surrounding regions: tectonic implications.* J. Geophyis. Res., **102**, 11863-11865.

NTC08 (Norme Tecniche per la Costruzione); 2008: *DM 140108, Ministero delle Infrastrutture.* Gazzetta Ufficiale, Roma.

Paolucci R. and Smerzini C.; 2010: *Strong ground motion in the epicentral region of the M_w 6.3, Apr. 6 2009, L'Aquila earthquake, Italy.* In: Proceedings of Fifth International Conference on Recent Advances in Geotechnical Earthquake Engineering and Soil Dynamics, San Diego, California, May 24-29, 2010.

Paolucci R., Pacor F., Puglia R., Ameri G., Cauzzi C. and Massa M.; 2010: *Record processing in ITACA, the new Italian strong-motion database.* In: Akkar S. and Gulkan P. (eds), Proceedings of 2nd Euro-Mediterranean meeting on Accelerometric Data Exchange and Archiving, Springer, in press.

Pino N.A. and Di Luccio F.; 2009: *Source complexity of the 6 April 2009 L'Aquila (central Italy) earthquake and its strongest aftershock revealed by elementary seismological analysis.* Geophys. Res. Lett., **36**, L23305, doi:10.1029/2009GL041331.

Somerville P.G., Smith N.F., Graves R.W. and Abrahamson N.A.; 1997: *Modification of empirical strong motion attenuation relations to include the amplitude and duration effect of rupture directivity.* Seismol. Res. Lett., **68**, 199–222.

Somerville P.G.; 2003: *Magnitude scaling of the near fault rupture directivity pulse.* Phys Earth Planet. In., **137**, 201–212.

Tothong P. and Luco N.; 2007:*Probabilistic seismic demand analysis using advanced ground motion intensity measures.* Earthquake Eng. Struct. Dyn., **36**, 1837–1860.

Zhu T.J., Heidebrecht A.C. and Tso W.K.; 1988: *Effect of peak ground acceleration to velocity ratio on ductility demand of inelastic systems.* Earthquake Eng. Struct. Dyn., **16**, 63–79.

Corresponding author: Gabriele Ameri
Istituto Nazionale di Geofisica e Vulcanologia
Via Bassini 15, 20133 Milano, Italy
Phone: +39 02 23699260; fax: +39 02 23699458; e-mail: ameri@mi.ingv.it